Synthesis of Well-Defined Polymer Brushes Grafted onto Silica Nanoparticles via Surface Reversible Addition−Fragmentation Chain Transfer Polymerization

Chunzhao Li and Brian C. Benicewicz*

NYS Center for Polymer Synthesis, Department of Chemistry and Chemical Biology, Rensselaer Polytechnic Institute, Troy, New York 12180

Received February 1, 2005; Revised Manuscript Received May 10, 2005

ABSTRACT: Reversible addition−fragmentation chain transfer polymerization (RAFT) was used to prepare polymer brushes grafted onto silica nanoparticles. Novel RAFT-silane agents were prepared that contained both an active RAFT moiety and a silane coupling agent. RAFT agents were anchored to silica nanoparticles by the functionalization of colloidal silica with the RAFT-silane agents. RAFT polymerizations were then conducted from the particle surface to graft homopolymer and block copolymer brushes to the particles. The kinetics of styrene (St) and *n*-butyl acrylate (*n*BuA) surface RAFT polymerizations were investigated and compared with model polymerizations mediated by free RAFT agent. The molecular weights of grafted polymers increased linearly with conversions, and first-order kinetics were observed in the conversion range studied, indicating that the surface graft polymerization proceeded in a controlled manner. Well-defined PSt-*block*-PBuA copolymers attached to silica nanoparticles were also prepared.

Introduction

Polymer nanocomposites are of great interest to both industry and academia due to the fascinating optical, magnetic, and electronic properties of particles at the nanoscale[1−4] and the exponential increase of particle surface area with the decrease in particle size.[3,4] The large surface area of nanoparticles has the ability to affect a large volume fraction of the matrix polymer. Therefore, interfacial interactions between nanoparticles and the matrix polymer are especially important in determining the properties of polymer nanocomposites.

Polymer grafting techniques provide a very versatile tool to tailor the surface of nanoparticles and thus the interfaces between nanoparticles and the matrix polymers. These techniques provide control over the type of polymer to be grafted onto the particle surface, surface densities, and chain lengths at the nanometer scale.[5] The techniques of covalently grafting polymer chains onto particles can be categorized into "grafting from" and "grafting to". The grafting to technique involves reacting the polymer, bearing an appropriate functional group, with the particles to chemically attach the polymer chains.[6,7] Because of the steric hindrance imposed by the already grafted chains, it becomes increasingly difficult for the incoming polymer chains to diffuse to the surface against the concentration gradient of the existing grafted polymers, which intrinsically results in low graft densities. In contrast, the grafting from technique uses initiators that have been initially anchored to the particle surface, followed by the polymerization from the surface. Since the existing grafted polymers will not hinder the diffusion of the small-sized monomers, significantly higher graft densities can be achieved with this technique.

Recently, the combination of surface-initiated polymerizations and controlled polymerization techniques has been widely explored as a route to design the surface properties and functionality of various substrates. Among the various types of polymerization methods, cationic,[8−10] anionic,[11,12] ring-opening metathesis,[13] and controlled radical polymerization methods[14−20] have all been used to graft polymers from different surfaces. Functionalized silica,[14,15,17,23,24] silicon wafer,[19,20] CdS,[21] and gold[16] have been used as substrates to initiate controlled polymerizations. Reversible addition−fragmentation chain transfer (RAFT) has recently emerged as a promising controlled radical polymerization technique due to its versatility and simplicity,[25−28] and the polymer is free from the contamination of metal catalyst. The RAFT technique is compatible with almost all of the conventional radical polymerization monomers. The polymerization conditions are similar to the conventional radical polymerization with the addition of a chain transfer agent (Z−(C=S)−SR) at the beginning of the reaction. Compared with the large number of reports using ATRP to prepare polymer brushes, there are surprisingly few reports on the application of RAFT techniques to the synthesis of polymer brushes, probably due to the difficulty of preparing RAFT agent anchored nanoparticles. With the convenient "grafting to" method, polymer grafted gold nanoparticles were prepared by the absorption of polymer bearing dithioester/thio end group which were synthesized by RAFT polymerization.[29−31] Baum et al. used AIBN-anchored silicates in the presence of free RAFT agents to synthesize polymer brushes grafted onto silicates.[32] Tsujii et al. prepared silica particles with attached RAFT agents using a multistep process.[33] First, an ATRP initiator was anchored onto the silica nanoparticles. Then, oligomeric PSt was grafted onto the ATRP functionalized particles. An atom transfer radical addition reaction was subsequently used to convert the terminal halogen to a dithio moiety. The resulting silica particles with anchored PSt macro-RAFT agents were used to mediate the controlled radical polymerization of styrene in the presence of additional free RAFT agent. Large amounts of free polymer were produced in the final products due to the free RAFT agent required in these two methods. Therefore, it is desirable to develop a new approach to directly anchor

10.1021/ma050216r CCC: $30.25
Published on Web 06/15/2005

RAFT agents to nanoparticle surfaces with high surface density and to prepare polymer grafted nanoparticles free from appreciable amounts of ungrafted polymer.

This paper reports the first synthesis of RAFT-silane coupling agents and their use to directly prepare RAFT agent anchored silica nanoparticles. The kinetics of styrene (St) and *n*-butyl acrylate (*n*BuA) graft polymerizations mediated by silica nanoparticles with anchored RAFT agents of varying surface density were examined and compared with the polymerizations mediated with free RAFT agents. Homopolymer and block copolymer grafted silica nanoparticles were also prepared and characterized.

Experimental Section

Materials. Tetrahydrofuran (99.9%, Acros) was dried over CaH_2 overnight and distilled before use. Styrene (99%, Acros) and *n*-butyl acrylate (99%, Acros) were passed through a basic alumina column to remove inhibitor and distilled under vacuum before use. Colloidal silica particles (D = 20 nm) of 30 wt % dispersed in methyl isobutyl ketone were kindly provided by Nissan Chemical. Allyl alcohol (99%), 2-bromopropionyl chloride (98%), and dimethylchlorosilane (96%) were purchased from Acros. The platinum(0)−1,3-divinyl-1,1,3,3-tetramethyldisiloxane complex (solution in xylene) and phenylmagnesium bromide (3.0 M in diethyl ether) were purchased from Aldrich. Unless otherwise specified, all chemicals were used as received.

Measurements. A Shimadzu GCMS-QP-5000 spectrometer equipped with SPB-5 column and EI source detector was used to identify reaction products and monitor the progress of the reaction. NMR spectra were recorded on a Varian 500 spectrometer using $CDCl_3$ as solvent. FT-IR spectra were measured by a BioRad Excalibur FTS3000. UV−vis absorption spectra were taken on a Perkin-Elmer Lamda 4C UV/vis spectrophotometer. Elemental analysis was conducted by Midwest Microlab (Indianapolis, IN). Molecular weights and molecular weight distributions were determined using a Waters gel-permeation chromatograph equipped with a 515 HPLC pump, 2410 refractive index detector, and three Styragel columns (HR1, HR3, and HR4 in the effective molecular weight range of 100−5000, 500−30 000, and 5000−500 000, respectively) with THF as eluent at 30 °C and a flow rate of 1.0 mL/min. The gel permeation chromatography (GPC) system was calibrated with polystyrene standards obtained from Polymer Labs with molecular weights ranging from 580 to 377 400. Thermal gravimetric analysis (TGA) was done on a Perkin-Elmer 7 series instrument with Pyris software. Sample was heated from 50 to 900 °C at 20 °C min^{-1} under a 20 mL min^{-1} dry N_2 flow. Transmission electron microscopic (TEM) observation was made on a JEOL transmission electron microscope JEM-1010 operated at 100 kV. The hydrodynamic radius of the particles was determined on a DynaPro-MS800 dynamic light scattering (DLS) instrument (Protein Solution, Lakewood, NJ) with a single detection angle at 90°. Particle hydrodynamic radius was calculated using Dynamics software (Protein Solutions).

Allyl 2-Bromopropionate. The synthesis of allyl 2-bromopropionate was carried out according to the methods in the literature.[12]

(3-(2-Bromopropionyl)propyl)dimethylchlorosilane (BPCS), 2. The platinum(0)−1,3-divinyl-1,1,3,3-tetramethyldisiloxane complex (0.5 mL) was added to a mixture of allyl 2-bromopropionate (94.3 mmol, 18.2 g) and dimethylchlorosilane (165 mmol, 15.1 g), and the reaction mixture was refluxed for 3 h. The completion of the hydrosilylation reaction was monitored by GC-MS with the disappearance of the allyl 2-bromopropionate peak. The excess dimethylchlorosilane was removed under vacuum, yielding a deep yellow oil. The oily residue was diluted with 20 mL of dried hexane and passed through a short column of anhydrous Na_2SO_4 to remove the catalyst. The obtained (3-(2-bromopropionyl)propyl)dimethylchlorosilane was used in the next step without further purification. GC-MS analysis showed that the reaction was nearly quantitative. ^{1}H NMR (500 MHz, $CDCl_3$): δ (ppm) 4.38 (q, 1H, J = 7.1, Br***C*****H**CH_3CO), 4.12−4.21 (m, 2H, COO***C*****H**$_2$-CH_2), 1.83 (d, 3H, J = 7.1, BrCH***C*****H**$_3CO$) 1.70−1.86 (m, 2H, $COOCH_2$***C*****H**$_2CH_2$), 0.85−0.89 (m, $COOCH_2CH_2$***C*****H**$_2$), 0.43 (s, (***C*****H**$_3)_2$ SiCl).

(3-(2-Bromopropionyl)propyl)dimethylmethoxysilane (BDMS), 3. BPCS (52.8 mmol, 15.2 g) was added dropwise to a mixture of methanol (54.7 mmol, 1.75 g) and pyridine (69.8 mmol, 5.52 g) in 150 mL of anhydrous ethyl ether at 0 °C. After complete addition, the solution was stirred overnight at room temperature. The solution was filtered to remove the pyridine salt. The filtrate was washed three times with 5% sodium bicarbonate solution and then dried over anhydrous magnesium sulfate overnight. After removal of solvent, the pale yellow product was used in the next step without further purification. ^{1}H NMR of the product did not show any signals attributable to the dimethylchlorosilane starting material. ^{1}H NMR (500 MHz, $CDCl_3$): δ (ppm) 4.34 (q, 1H, J = 6.8, Br***C*****H**CH_3CO), 4.05−4.15 (m, 2H, COO***C*****H**$_2$-CH_2), 3.4 (s, 3H, $(CH_3)_2$ SiO***C*****H**$_3$), 1.80 (d, 3H, J = 6.8, BrCH***C*****H**$_3CO$), 1.65−1.72 (m, $COOCH_2$***C*****H**$_2CH_2$), 0.59−0.63 (m, $COOCH_2CH_2$***C*****H**$_2$), 0.10 (s, (***C*****H**$_3)_2$ $SiOCH_3$).

(3-(2-Dithiobenzoatepropionyl)propyl)dimethylmethoxysilane, RAFT-Silane Agent, 4. Phenylmagnesium bromide (5 mL, 3 M solution in ethyl ether) was added to a 100 mL round-bottom flask and diluted to 20 mL with anhydrous THF. Carbon disulfide (15.8 mmol, 1.23 g) was added dropwise to this mixture and stirred for 0.5 h at room temperature. (3-(2-Bromopropionyl)propyl)dimethylmethoxysilane (BDMS), **3** (19 mmol, 5.3 g), was added dropwise to the dark red solution, and the mixture was stirred for another 6 h. Water was added to the mixture, and the organic product was extracted with diethyl ether (3 × 50 mL), then dried with anhydrous magnesium sulfate overnight, and filtered. After removal of solvent and purification via silica gel column chromatography (5:1 mixture of hexane and ethyl ether), pure RAFT-silane **4** was obtained as a red oil (2.02 g, 38% yield). ^{1}H NMR (500 MHz, $CDCl_3$): δ (ppm) 7.97−8.00 (d, 2H, aromatic ring), 7.50−7.53 (t, 1H, aromatic ring), 7.35−7.38 (t, 2H, aromatic ring), 4.75 (q, 1H, J = 7.4, S***C*****H**CH_3CO), 4.05−4.18 (m, 2H, COO***C*****H**$_2CH_2$), 3.4 (s, 3H, $(CH_3)_2$ SiO***C*****H**$_3$), 1.68 (d, 3H, J = 7.4, SCHC***H***$_3CO$), 1.66−1.74 (m, $COOCH_2$***C*****H**$_2CH_2$), 0.59−0.63 (m, $COOCH_2CH_2$***C*****H**$_2$), 0.10 (s, (***C*****H**$_3)_2$ $SiOCH_3$). ^{13}C NMR (125 MHz, $CDCl_3$): δ (ppm) 226.2 (***C***=S), 171.4 (***C***=O), 144.6, 132.9, 128.6, 127.2, 68.3, 50.5, 48.8, 22.6, 16.7, 11.9, −2.5. IR (NaCl disk): 2954, 1735 (C=O), 1046 cm^{-1} (C=S). Anal. Calcd: C, 53.93%; H, 6.74%; S, 17.98%. Found: C, 54.12%; H, 6.59%; S, 18.03%.

General Procedure for RAFT Agent Immobilization Reaction. Colloidal silica particle suspension (48 mL of 30 wt % SiO_2 in MIBK, D 20 nm), **4** (1.7 mmol, 0.61 g), and dried THF (6 mL) were added to a three-neck round-bottom flask. The reaction mixture was heated at 85 °C under N_2 protection overnight and then cooled to room temperature. The reaction mixture was then precipitated into a large amount of hexanes (500 mL). The particles were recovered by centrifugation at 3000 rpm for 15 min. The particles were then redissolved in 20 mL of acetone and reprecipitated in 200 mL of hexanes again. This dissolution−precipitation procedure was repeated another three times until the supernatant layer after centrifugation was colorless. The red RAFT agent anchored nanoparticles **5** were dried at room temperature (13.4 g, 93% yield).

Styrene Graft Polymerization from RAFT Agent Anchored Silica Nanoparticles. RAFT agent anchored silica (0.108 g, 69 μmol/g), THF (1 mL), and styrene (7.6 mmol, 0.88 mL) were added to a 15 mL Schlenk tube. After sonication for 1 min, AIBN (8.0 μL of 0.050 M THF solution, [AIBN]/[RAFT] = 0.053) was added. The tube was subjected to three cycles of freeze−pump−thaw to remove oxygen. The tube was then placed in an oil bath preset to 65 °C for various intervals. The polymerization was stopped by quenching the tube in ice water, and the polymerization mixture was poured into an aluminum boat to evaporate the solvent in a fume hood. The

Scheme 1. Synthesis Procedures for Attaching RAFT Agent onto Silica Nanoparticles

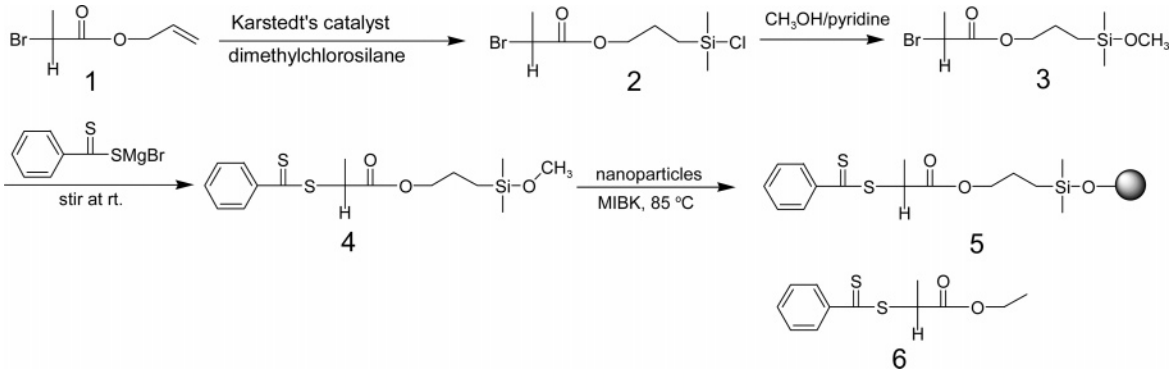

aluminum boat was then transferred to a vacuum oven to remove traces of solvent and monomer at 30 °C overnight to determine the monomer conversions via gravimetry. A monomer conversion of 12% was reached after 24 h. The cleaved PSt had a number-average molecular weight of 15 300 and a PDI of 1.08.

Butyl Acrylate Graft Polymerization from RAFT Agent Anchored Silica Nanoparticles. RAFT agent anchored silica (0.201 g, 69 μmol/g) and *n*-butyl acrylate (6.9 mmol, 1 mL) were added to a 15 mL Schlenk tube. After sonication for 1 min, AIBN (21.0 μL of 0.050 M THF solution, [AIBN]/[RAFT] = 0.076) was added. The tube was subjected to three cycles of freeze−pump−thaw to remove oxygen. The tube was then placed in an oil bath preset to 70 °C for various intervals. The polymerization was stopped by quenching the tube in ice water, and the polymerization mixture was poured into an aluminum boat to evaporate the solvent in a fume hood. The aluminum boat was then transferred to a vacuum oven to remove traces of solvent and monomer at 30 °C overnight to determine the monomer conversion via gravimetry. A monomer conversion of 18% was reached after 9 h. The cleaved PBuA had a number-average molecular weight of 16 000 and a PDI of 1.08.

Synthesis of SiO_2-*graft*-(PBuA-*block*-PSt). SiO_2-*graft*-PBuA (0.1 g), styrene (130 mmol, 1.50 mL), and toluene (1.5 mL) were added to a 15 mL Schlenk tube. The tube was subjected to three cycles of freeze−pump−thaw to remove oxygen. The tube was then placed in an oil bath preset to 100 °C for 3 h. The polymerization was stopped by quenching the tube in ice water, and the polymerization mixture was poured into an aluminum boat to evaporate the solvent in fume hood. The aluminum boat was then transferred to a vacuum oven to remove traces of solvent and monomer at 30 °C overnight to determine the monomer conversion via gravimetry. A monomer conversion of 10% was reached after 3 h. The cleaved PSt-*block*-PBuA had a number-average molecular weight of 32 000 and a PDI of 1.14.

General Procedures for Cleaving Grafted Polymer from Particles. Generally phase transfer agent Aliquat 336 was required to transfer the HF in the aqueous phase to the organic phase to efficiently etch the silica of polymer grafted silica particles.[14] In this work, a slightly modified procedure was used to cleave the polymer from the silica nanoparticles. In the modified procedure, a relatively large amount of THF was used as the cosolvent for both the polymer grafted silica and HF(aq) solution. Phase transfer agent Aliquat 336 was not used since it has a GPC molecular weight of ≈1000 which will overlap with the low molecular weight polymer fraction, thereby complicating the molecular weight and polydispersity calculations.

In a typical experiment, polystyrene (50 mg) grafted silica particles were dissolved in THF (3 mL). HF (0.2 mL, 49% in aq) was added, and the solution was allowed to stir at room temperature overnight. The solution was poured into a PTFE Petri dish and allowed to stand in a fume hood overnight to evaporate the volatiles. The recovered PSt was then subjected to GPC analyses. Similar procedures were used to recover PBuA and block copolymers.

Results and Discussion

RAFT-Silane Coupling Agent. One of the goals of this work was to attach the RAFT agent directly to the nanoparticle surface. In general, attachment of the RAFT agent to nanoparticles can be accomplished through either the Z or R group. Mayadunne et al. compared polymerizations mediated by two star RAFT agents, independently attached to the core through the Z and R groups and demonstrated that the star RAFT agent attached to the core through the Z group produced star polymer free from star−star coupling.[34] However, this methodology may not be applicable to the preparation of polymer brushes grafted onto nanoparticles. If the Z group of a RAFT agent was attached to a nanoparticle, the chain transfer reactions between free polymeric radicals and attached polymeric RAFT agents would occur near the surface of the particle. Steric hindrance of the attached polymer chains could severely limit the efficiency of this chain transfer reaction, therefore leading to a loss of control over the molecular weight and polydispersity. The mechanistic similarities between star RAFT agents attached to the core through the Z group and the "grafting to" technique, and the intrinsic difficulties of the "grafting to" technique as discussed above prompted us to design RAFT agents anchored onto silica nanoparticles through the R group moiety. The synthesis of a dithioester compound also containing a dimethylmethoxysilane (RAFT-silane) headgroup, **4**, is shown in Scheme 1. The methoxysilane group was used to anchor the dithioester to the substrates, thus leaving the pendant dithioester to mediate the RAFT polymerization. The reaction first involved the synthesis of allylic α-bromoester **1**, which was followed by the hydrosilylation reaction to prepare compound **2** with a chlorosilane headgroup. Reaction of **2** with methanol converted the highly reactive chlorosilane to the more stable methoxysilane compound **3** capable of withstanding the conditions of the subsequent reactions. This silane agent **3** was then reacted with bromomagnesium dithiobenzoate to prepare the desired RAFT-silane agent **4** with a purified yield of 38%. This yield was lower than the model reaction of the dithiosalt with ethyl bromoisopropyrate (62% yield, **6**), which could be attributed to the instability of the methoxysilane group or the absorption to silica gel during column chromatography.

Nanoparticle Functionalization. The silane coupling reaction was conducted by heating the RAFT-silane agent **4** with colloidal silica particles dispersed in methyl isobutyl ketone (MIBK) at 85 °C overnight. Subsequent dispersion of the modified particles in acetone followed by precipitation in hexane and cen-

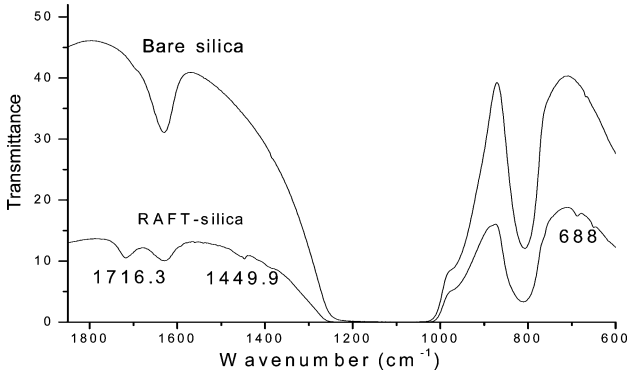

Figure 1. FT-IR spectra (KBr pellet) of bare silica nanoparticles and RAFT agent anchored silica nanoparticles.

trifugation steps were used to remove the unreacted RAFT-silane and side products such as the dimerized RAFT-silane product. Since the side products and unreacted RAFT-silane agent were all red compounds, it was very easy to determine whether the modified silica nanoparticles were purified by simply observing the color of the supernatant after centrifugation. Generally, the supernatant was colorless after three such dispersion−precipitation−centrifugation cycles, which indicated the modified silica nanoparticles were free from unattached RAFT agents. During the submission of this work, Skaff et al. reported the synthesis of trithiocarbonate functionalized cadium selenide nanoparticles via ligand coordination and polymerizations using such particles.[35]

Figure 1 shows the partial FT-IR spectra of the bare silica and RAFT agent anchored silica. Characteristic absorption bands were clearly visible at 1716.3 cm^{-1} due to the carbonyl group and at 1449.9 and 688 cm^{-1} due to the phenyl ring. The thiocarbonyl absorption at 1120 cm^{-1} was not observed due to the overlap with the strong absorption of bare silica. The attachment of the RAFT-silane agent **4** onto silica nanoparticles was also confirmed by UV−vis spectra. The structurally similar RAFT agent **6** showed absorptions at 300 and 228 nm due to the dithiobenzoyl group and ester group, respectively. After the immobilization reaction, the ultraviolet−visible spectra of the RAFT agent anchored silica particles revealed very similar absorption bands at 300 and 228 nm. The amount of RAFT agent on the modified silica nanoparticles was determined quantitatively by comparing the absorption at 300 nm for the RAFT agent anchored silica nanoparticles **5** to a standard absorption curve made from known amounts of the free RAFT agent **6**.

To investigate the effect of surface density of the anchored RAFT agents on the controlled radical polymerization behavior, silica nanoparticles with different RAFT agent graft densities were prepared by systematically varying the ratio of the amounts of RAFT-silane agent and silica particles in the reactions. The amount of RAFT agent attached to the particle surface ranged from 37 to 171 μmol/g as determined by UV−vis spectroscopy. RAFT agent surface densities (number of RAFT agents/nm^2) were calculated using a similar procedure reported by Pyun et al.[17] with the assumption that the density of RAFT agent anchored silica nanoparticles was comparable to that of bulk silica (2.07 g/cm^3). Figure 2 shows the graft densities of RAFT agent vs the concentration of the RAFT-silane agent **4** used in the reaction. It can be seen that surface coverage of

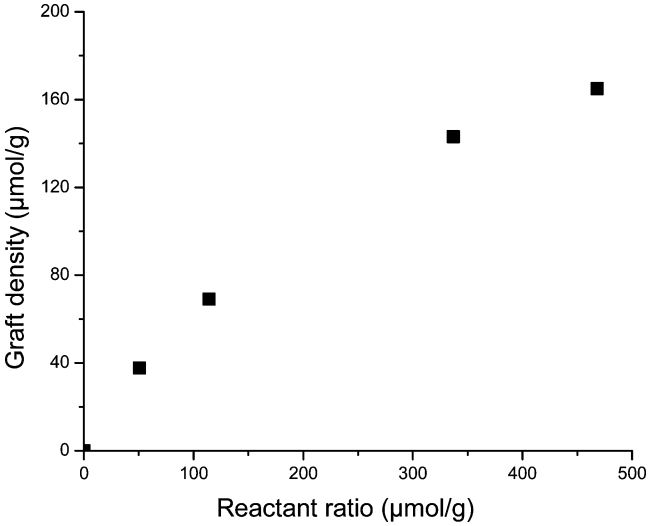

Figure 2. Graft densities of SiO_2−RAFT **5** as a function of the silane concentration (μmol of RAFT-silane/g of silica nanoparticle) utilized for deposition. The silane concentration is given in the same units as the graft density.

the particles with RAFT agents can be varied in a controlled manner from 0.15 to 0.68 RAFT agents/nm^2. These silica particles with various RAFT agent surface densities, therefore, can be used to prepare thinly to densely populated polymer grafted nanoparticles.

Homopolymerization. To minimize polymeric radical recombination due to the reported "surface radical migration" effect,[33] particles with low RAFT agent surface density (69 μmol/g, 0.28 RAFT agents/nm^2) and low AIBN/CTA ratio (0.053 for styrene) were utilized. The polymerizations were conducted at low conversion range (<20%) to avoid possible gelation or interparticle polymeric radical coupling.[17] These measures will also help to reduce the amount of free polymer derived from the radicals formed by AIBN decomposition, which is influenced by the AIBN/CTA ratio, AIBN initiation efficiency, and monomer conversion. Styrene radical polymerization mediated by the free RAFT agent, ethyl *S*-thiobenzoyl-2-thiopropionate (**6**), was also conducted at the identical conditions for comparison. The results of the kinetic studies for styrene polymerization mediated by RAFT agent anchored silica nanoparticles **5** (two graft densities) and free RAFT agent **6** are shown in Figure 3. The graph shows an almost linear relationship between monomer consumption and time for both cases over the conversion range studied, which indicates a constant free radical concentration during the polymerization. However, the polymerizations mediated by anchored RAFT agent **5** were apparently slower than the model polymerization mediated by free RAFT agent **6** at identical conditions. Similar features were also observed for the polymerization of *n*-butyl acrylate mediated by RAFT agent anchored silica nanoparticles **5** at 70 °C with an AIBN/CTA ratio of 0.076 (Figure 4). After an induction period of approximately 2−3 h, monomer conversion increased linearly with time. Again, the model polymerization mediated with free RAFT agent **6** showed an apparently higher polymerization rate and no induction period. The polymerization retardations for RAFT polymerization have been observed and discussed extensively.[36−42] It was postulated to be due to the slow fragmentation of the intermediate polymeric radical[36−38,41] or irreversible intermediate polymeric radical termination.[39,42] This retardation ef-

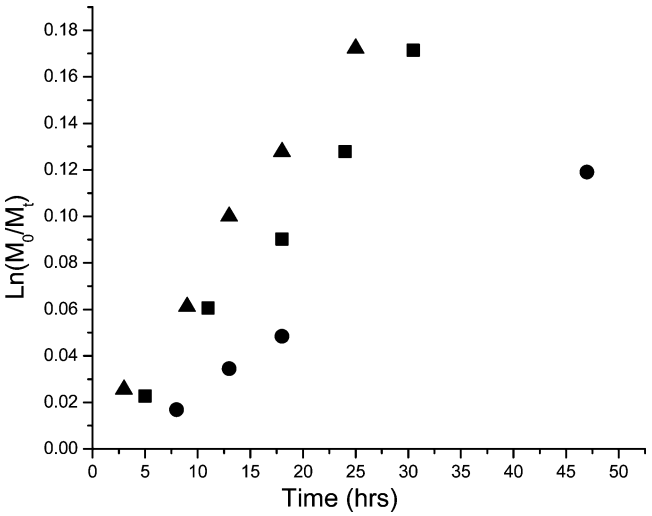

Figure 3. Pseudo-first-order rate plot for the polymerization of styrene (4.1 M in THF) with AIBN as initiator (2.1×10^{-4} M) mediated with RAFT agent anchored silica nanoparticles **5** (4×10^{-3} M; square, 69 μmol/g; circle, 171 μmol/g) and **6** (4×10^{-3} M, triangle). [AIBN]/[CTA] ratio was 0.053 for all polymerizations.

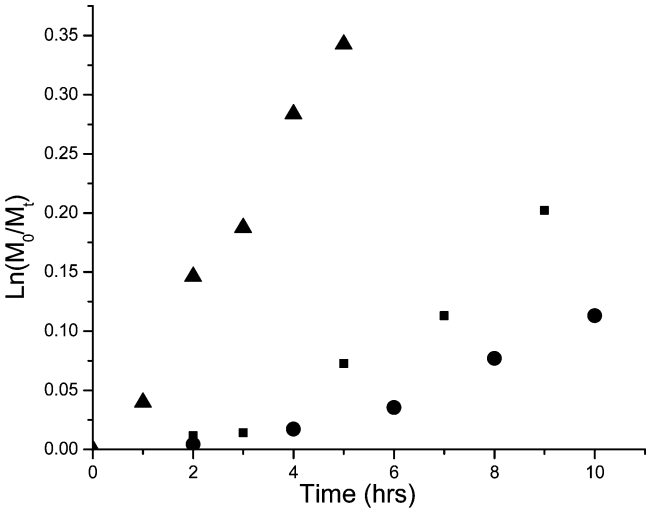

Figure 4. Pseudo-first-order rate plot for the polymerization of *n*-butyl acrylate (6.9 M) with AIBN as initiator (1.05×10^{-3} M) mediated with RAFT agent anchored silica nanoparticles **5** (1.38×10^{-2} M; square, 69 μmol/g; circle, 165 μmol/g) and **6** (1.38×10^{-2} M, triangle). [AIBN]/[CTA] ratio was 0.076 for all polymerizations.

fect was also found to be dependent on RAFT agent concentration and became more pronounced with increasing RAFT agent concentration.[40] One key difference between surface anchored RAFT agent and the free RAFT agent mediated polymerizations is the localized concentration of RAFT agent. For the free RAFT agent mediated polymerization, the RAFT agents were distributed homogeneously throughout the reaction solution, and thus a constant RAFT agent concentration was maintained throughout the solution. However, in the case of surface anchored RAFT agents, the local concentration of RAFT agent on the nanoparticle surfaces was very high due to the immobilization of the RAFT agents. For the 69 μmol/g anchored RAFT agent nanoparticles, the concentration of the RAFT agent in the volume of the surface layer extending 1 nm from the surface of the nanoparticle is calculated to be 0.42 M, which is more than 1 order higher than the normally used RAFT agent concentration ($\sim 10^{-2}$ M) for polymerization. Once a

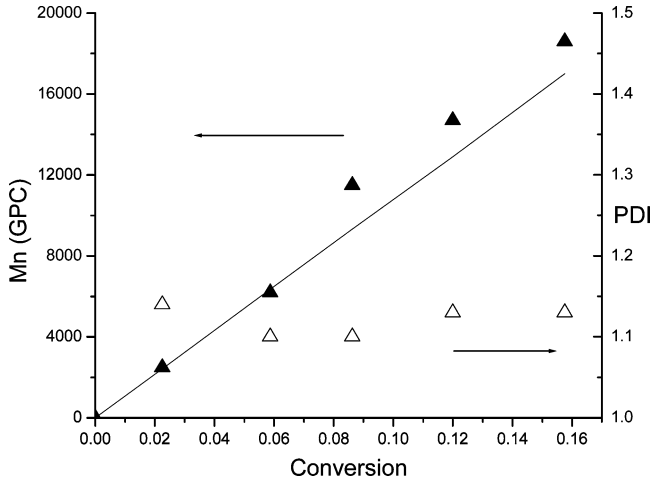

Figure 5. Dependence of molecular weight (solid line, $M_{n,theory}$) and polydispersity on conversion for styrene polymerization in the presence of RAFT agent anchored silica nanoparticles **5** (69 μmol/g).

radical in solution is transferred to the nanoparticle surface via a chain transfer reaction, the radical will prefer to degeneratively transfer to a nearby RAFT agent rather than propagate due to the locally high RAFT agent concentration, therefore leading to a more pronounced polymerization retardation compared with the free RAFT agent mediated polymerization. It can also be reasoned from the discussion above that the polymerization will be more retarded with increasing surface concentration of the anchored RAFT agent. Therefore, polymerization kinetics experiments of styrene mediated with higher surface density RAFT agent anchored silica nanoparticles (171 μmol/g) were conducted at the identical conditions ([AIBN]/[CTA] of 0.053). Indeed, it was observed that the polymerization rate was apparently lower than the low surface density RAFT agent anchored nanoparticles (69 μmol/g) and free RAFT agent mediated polymerization (Figure 3). The same polymerization rate trend was also followed by *n*-butyl acrylate polymerization as shown in Figure 4.

The controlled character of the styrene graft polymerization was demonstrated by the results in Figure 5, which showed that the number-average molecular weight increased linearly with monomer conversion, measured molecular weights were in general agreement with theoretical molecular weights, and molecular weight distributions were generally very narrow (<1.2). These data showed that the anchored RAFT agents participated in the polymerization with a high activity (defined as the ratio of $M_{n,theoretical}$ and $M_{n,GPC}$)[17] of 80% and were not hindered by their attachment to the nanoparticle surfaces. In previous work on the graft polymerization of styrene from nanoparticle surfaces using RAFT, considerable low molecular weight tailing and high molecular weight humps were observed.[33] This was attributed to the surface radical migration effect and termination by recombination. In our work, only slight amounts of high molecular weight chains were observed in the GPC curves of the cleaved PSt at 12% monomer conversion (Figure 6). This could be ascribed to the low AIBN/CTA ratio (0.053), low polymerization temperature (65 °C), and low RAFT agent surface density utilized for the polymerization which resulted in a low probability of polymeric radical termination by combination. The molecular weight of the cleaved PBuA also increased linearly with conversions and molecular

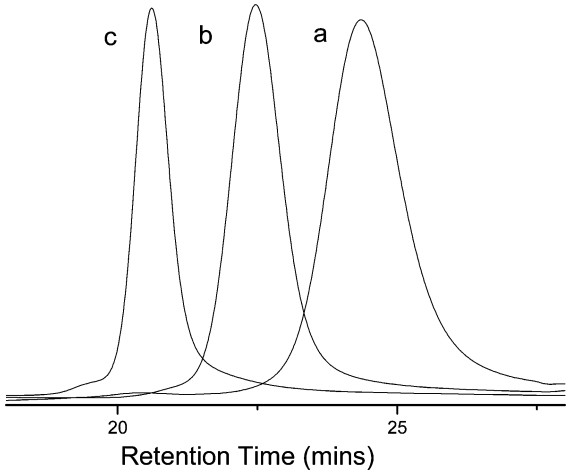

Figure 6. GPC traces of cleaved polystyrene of styrene graft polymerization in THF for (a) 2.2% conversion, M_n = 2500; (b) 5.8% conversion, M_n = 6200; (c) 12% conversion, M_n = 15 200; [St] = 4.1 M, [AIBN] = 2.1×10^{-4} M, [**5**] = 4×10^{-3} M.

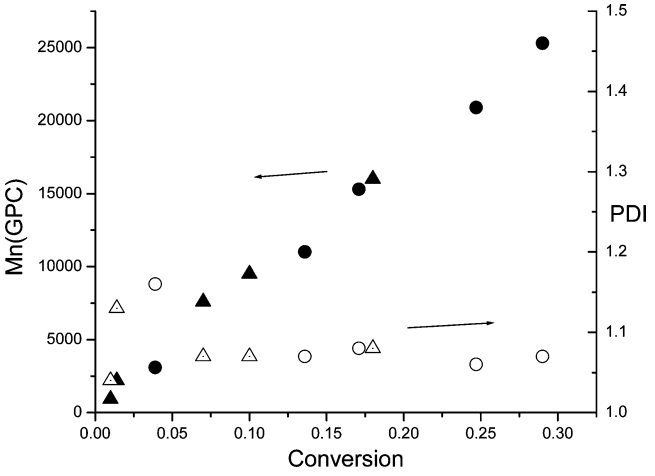

Figure 7. Dependence of molecular weight and polydispersity on conversion for *n*-butyl acrylate polymerization in the presence of RAFT agent anchored silica nanoparticles **5** (triangle, 69 μmol/g) and free RAFT agent **6** (circle).

weight distributions were generally very narrow (<1.15). Although the accurate molecular weight of the grafted PBuA cannot be determined by GPC calibrated with PSt or PMMA standards, a comparison of the plot of $M_{n,GPC}$ vs conversion between the anchored RAFT agent system and free RAFT agents system targeting the same molecular weight could be used to evaluate the relative activity of the anchored RAFT agents. The results of these polymerizations (Figure 7) show that the molecular weights and polydispersities were unaffected by the surface attachment of the RAFT agent. This clearly demonstrated that the ability of the anchored RAFT agent to control the molecular weight and polydispersity for BuA polymerization was comparable to the free RAFT agent. GPC traces of the cleaved PBuA were generally symmetrical up to 18% monomer conversion, and significant high molecular weight humps or low molecular weight tailing were not observed (Figure 8). These results showed that the extensive "surface radical migration" of RAFT polymerization could be relieved by using the approach outlined in this paper.

Although determination of the amount of ungrafted polymer will be discussed in detail in a future paper, preliminary work with as-prepared PSt grafted fumed

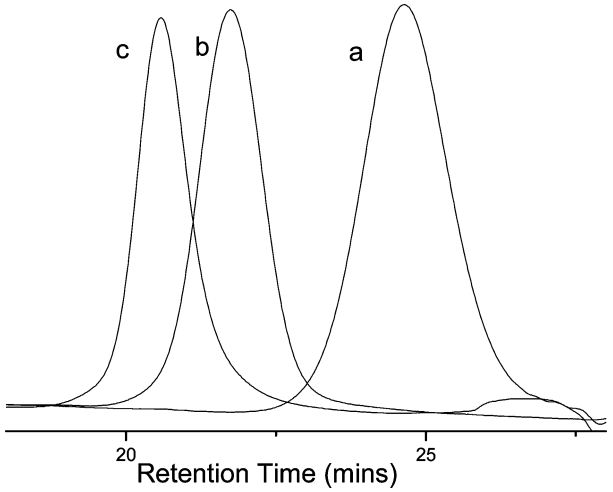

Figure 8. GPC traces of cleaved PBuA of *n*-butyl acrylate graft polymerization in THF for (a) 1.4% conversion, M_n = 2200; (b) 7% conversion, M_n = 7600; (c) 18% conversion, M_n = 16 000; [*n*-BuA] = 6.9 M, [AIBN] = 1.05×10^{-3} M, [**5**] = 1.38×10^{-2} M.

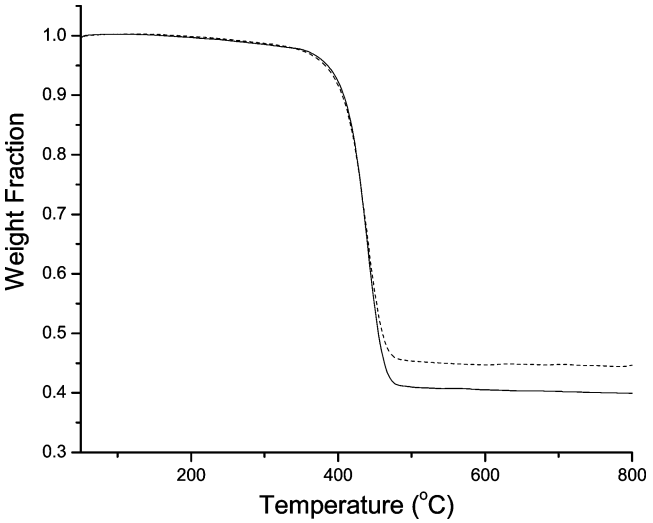

Figure 9. TGA analysis of as-prepared PSt grafted fumed silica (solid line) and purified PSt grafted fumed silica (dash line).

silica (M_n 13 200, PDI 1.26, conversion 16.6%) showed that the fraction of ungrafted polymer estimated by TGA (Figure 9) was only 9% after the particles were thoroughly washed with toluene by two repeated cycles of dispersion−centrifugation (10 000 rpm for 1 h). We conclude that the immobilization of the RAFT agent onto silica nanoparticles is an efficient method for preparing polymer brushes on nanoparticle surfaces.

Block Copolymerization. With controlled radical polymerization methods, both homopolymers and block copolymers can be grafted onto the particle surface. For the design of nanocomposite properties, the outer block could be the block compatible with a polymer matrix, and the inner block could be designed with specific interphase properties. The chain extension to form block copolymers could also be used as a qualitative indication of the "livingness" of the homopolymer grafted from the particle surface.

In the chain extension experiments, PBuA homopolymer grafted silica nanoparticles were first prepared with a monomer conversion of 9.8% (8 h, 70 °C). The cleaved polymer had a number-average molecular weight (GPC)

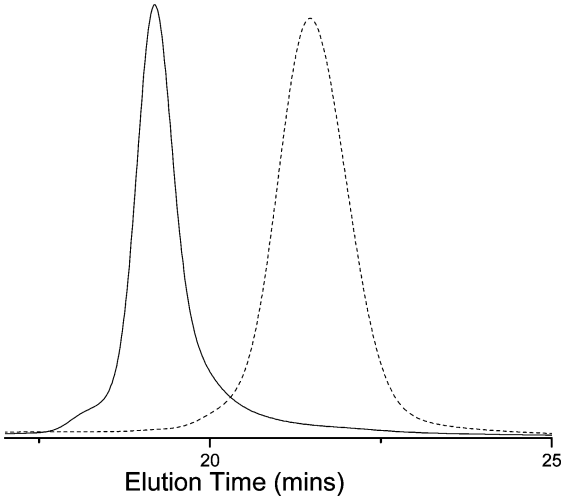

Figure 10. GPC traces for polymer from SiO_2-*graft*-PBuA and SiO_2-*graft*-(PBuA-*block*-PSt), cleaved PBuA (dotted line, M_n = 10 500, PDI = 1.09) and cleaved PBuA-*block*-PSt (solid line, M_n = 32 000, PDI = 1.14).

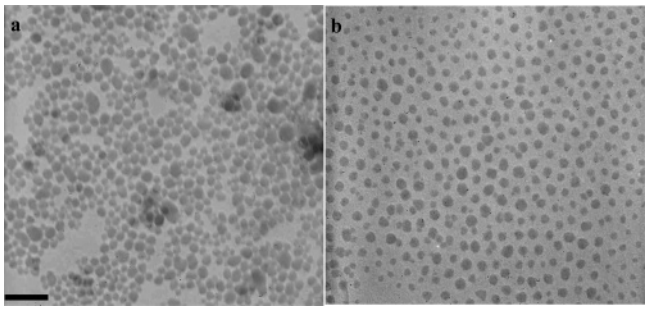

Figure 11. TEM images of bare (a) silica nanoparticles and (b) PBuA grafted silica nanoparticles.

of 10 500 and a PDI of 1.09. The isolated PBuA grafted silica nanoparticles bearing a dithioester end group were then used as macro-RAFT agents for the chain extension with styrene to prepare P(St-*block*-BuA)-*graft*-SiO_2. The styrene conversion was 10% after 3 h at 100 °C. The final cleaved PSt-*block*-PBuA had a number-average molecular weight of 32 000 and a PDI of 1.14. The complete shift of the GPC trace (Figure 10) and low polydispersity (PDI = 1.14) of the final block copolymer again demonstrated the "livingness" of the PBuA macro-RAFT agents grafted onto silica nanoparticles and a very high reinitiation efficiency of the macro-RAFT agents. The small high molecular weight hump observed for the block copolymer could be attributed to the recombination of polystyrene radicals, as seen in the polystyrene homopolymers. DLS experiments of the particles in dilute THF solution also confirmed an increase of particle size for PBuA-*graft*-SiO_2 (D = 46 nm) compared with the bare silica nanoparticle (D = 20 nm). Although it is desirable to obtain the size of P(St-*block*-BuA)-*graft*-SiO_2, the interparticle termination of the polystyrene radicals as shown in the GPC trace (Figure 10) made it difficult to prepare a clean solution for light scattering experiments.

Characterization of the Grafted Nanoparticles. TEM was used to characterize the morphology of the polymer grafted silica nanoparticles. Thin layers of PBuA grafted silica nanoparticles were prepared by casting a drop of dilute suspension of grafted nanoparticles in THF onto a copper grid and evaporating the solvent. Figure 11a shows the TEM image of the silica nanoparticles with the RAFT agent attached to the surface which agglomerated after solvent evaporation. Figure 11b shows the TEM image of PBuA (M_n 22 400, PDI 1.15) grafted silica nanoparticles. It clearly revealed that the particles were well dispersed in the matrix of poly(butyl acrylate) brushes, and no silica particle agglomerates were observed. The distance between particles was much larger than the distance between RAFT agent anchored silica nanoparticles, and this distance was determined by the molecular weight of homo-poly(butyl acrylate) brushes.

Conclusions

A general scheme for the design and synthesis of RAFT-silane agents was proposed. The first RAFT-silane agent was prepared which was used to directly attach a RAFT agent to the surface of silica nanoparticles. The surface density of the RAFT agent could be controlled by the ratio of reactants in the functionalization reaction. Controlled radical polymerizations were conducted that produced narrow polydispersity polymers with predictable molecular weights without the need for additional free RAFT agent. Preliminary results showed that this approach for grafting polymer chains onto nanoparticles resulted in high (>80%) graft efficiency. The kinetics of St and *n*BuA surface polymerizations mediated by the RAFT agent anchored silica nanoparticles with two different surface densities were investigated and compared with model polymerizations mediated by free RAFT agents. Polymerization retardation was observed for the surface anchored RAFT agent mediated polymerization and was ascribed to the locally high RAFT agent concentration near the particle surface. Despite the retardation effect, well-defined PSt and PBuA grafted nanoparticles could be prepared by the polymerization mediated by the surface anchored RAFT agent. The synthesis of polymer brushes grafted onto silica nanoparticles was confirmed by TEM analysis which showed that the particles were homogeneously functionalized with polymer chains. Poly(St-*block*-BuA) copolymers grafted onto silica nanoparticles could be prepared from the poly(BuA-*graft*-SiO_2) macro-RAFT agent.

Acknowledgment. The authors thank Eastman Kodak Company for their generous financial support through the Nanoscale Science and Engineering Initiative of the National Science Foundation under NSF Award DMR-0117792.

References and Notes

(1) Alivisatos, A. P. *Science* **1996**, *271*, 933−937.
(2) Golden, J. H.; Deng, H. B.; Disalvo, F. J.; Thompson, P. M.; Frechet, J. M. *Science* **1995**, *268*, 1463−1466.
(3) Ash, B. J.; Siegel, R. W.; Schadler, L. S. *Macromolecules* **2004**, *37*, 1358−1369.
(4) Ash, B. J.; Rogers, D. F.; Wiegand, C. J.; Schadler, L. S.; Siegel, R. W.; Benicewicz, B. C.; Apple, T. *Polym. Compos.* **2002**, *23*, 1014−1025.
(5) Prucker, O.; Ruhe, J. *Macromolecules* **1998**, *31*, 592−601.
(6) Tsubokawa, N.; Machida, S.; Yoshikawa, S. *J. Polym. Sci., Polym. Chem.* **2002**, *36*, 3165−3172.
(7) Yoshikawa, J.; Tsubokawa, N. *Polym. J.* **1996**, *28*, 317−322.
(8) Zhao, B.; Brittain, W. J.; Zhou, W.; Cheng, S. Z. D. *J. Am. Chem. Soc.* **2000**, *122*, 2407−2408.
(9) Vidal, A.; Guyot, A.; Kennedy, J. P. *Polym. Bull. (Berlin)* **1982**, *6*, 401−407.
(10) Vidal, A.; Guyot, A.; Kennedy, J. P. *Polym. Bull. (Berlin)* **1980**, *2*, 315−327.

(11) Jordan, R.; Ulman, A. *J. Am. Chem. Soc.* **1998**, *120*, 243−247.
(12) Jordan, R.; Ulman, A.; Kang, J. F.; Rafailovich, M. H.; Sokolov, J. *J. Am. Chem. Soc.* **1999**, *121*, 1016−1022.
(13) Juang, A.; Scherman, O. A.; Grubbs, R. H.; Lewis, N. S. *Langmuir* **2001**, *17*, 1321−1323.
(14) von Werne, T.; Patten, T. E. *J. Am. Chem. Soc.* **1999**, *121*, 7409−7410.
(15) von Werne, T.; Patten, T. E. *J. Am. Chem. Soc.* **2001**, *123*, 7497−7505.
(16) Ohno, K.; Koh, K.; Tsujii, Y.; Fukuda, T. *Macromolecules* **2002**, *35*, 8989−8993.
(17) Pyun, J.; Jia, S.; Kowalewski, T.; Patterson, G. D.; Matyjaszeswski, K. *Macromolecules* **2003**, *36*, 5094−5104.
(18) Carrot, G.; Diamanti, S.; Manuszak, M.; Charleux, B.; Vairon, J.-P. *J. Polym. Sci., Part A: Polym. Chem.* **2001**, *39*, 4294−4301.
(19) Matyjaszewski, K.; Miller, P. J.; Shukla, N.; Immaraporn, B.; Gelman, A.; Luokala, B. B.; Siclovan, T. M.; Kickelbick, G.; Vallant, T.; Hoffmann, H.; Pakula, T. *Macromolecules* **1999**, *32*, 8716−8724.
(20) Jeyaprakash, J. D.; Samuel, S.; Dhamodharan, R.; Ruhe, J. *Macromol. Rapid Commun.* **2002**, *23*, 277−281.
(21) Carrot, G.; Rutot-Houze, D.; Pottier, A.; Degee, P.; Hilborn, J.; Dubois, P. *Macromolecules* **2002**, *35*, 8400−8404.
(22) Pyun, J.; Matyjaszewski, K.; Kowalewski, T.; Savin, D.; Patterson, G.; Kickelbick, G.; Huesing, N. *J. Am. Chem. Soc.* **2001**, *123*, 9445−9446.
(23) Ohno, K.; Morinaga, T.; Koh, K.; Tsujii, Y.; Fukuda, T. *Macromolecules* **2005**, *38*, 2137−2142.
(24) Savin, D. A.; Pyun, J.; Patterson, G. D.; Kowalewski, T.; Matyjaszewski, K. *J. Polym. Sci., Part B: Polym. Phys.* **2002**, *40*, 2667−2676.
(25) Le, T. P.; Moad, G.; Rizzardo, E.; Thang, S. H. PCT Int. Appl. WO 9801478, 1998.
(26) Ladaviere, C.; Dorr, N.; Claverie, J. P. *Macromolecules* **2001**, *34*, 5370−5372.
(27) Kanagasabapathy, S.; Sudalai, A.; Benicewicz, B. C. *Macromol. Rapid Commun.* **2001**, *22*, 1076−1080.
(28) Li, C.; Benicewicz, B. C. *J. Polym. Sci., Part A: Polym. Chem.* **2005**, *43*, 1058−1063.
(29) Lowe, A. B.; Sumerlin, B. S.; Donovan, M. S.; McCormick, C. L. *J. Am. Chem. Soc.* **2002**, *125*, 11562−11563.
(30) Shan, J.; Nuopponen, M.; Jiang, H.; Kauppinen, E.; Tenhu, T. *Macromolecules* **2003**, *36*, 4526−4533.
(31) Matsumoto, K.; Tsuji, R.; Yonemushi, Y.; Yoshida, T. *J. Nanoparticle Res.* **2004**, *6*, 649−659.
(32) Baum, M.; Brittain, W. J. *Macromolecules* **2002**, *35*, 610−615.
(33) Tsujii, Y.; Ejaz, M.; Sato, K.; Goto, A.; Fukuda, T. *Macromolecules* **2001**, *34*, 8872−8878.
(34) Mayadunne, R. T. A.; Jeffery, J.; Moad, G.; Rizzardo, E. *Macromolecules* **2003**, *36*, 1505−1513.
(35) Skaff, H.; Emrick, T. *Angew. Chem., Int. Ed.* **2004**, *43*, 5383−5386.
(36) Barner-Kowollik, C.; Vana, P.; Quinn, J. F.; Davis, T. P. *J. Polym. Sci., Polym. Chem.* **2002**, *40*, 1058−1063.
(37) Barner-Kowollik, C.; Quinn, J. F.; Nguyen, T. L. U.; Heuts, J. P. A.; Davis, T. P. *Macromolecules* **2001**, *34*, 7849−7857.
(38) Barner-Kowollik, C.; Quinn, J. F.; Morsley, D. R.; Davis, T. P. *J. Polym. Sci., Polym. Chem.* **2001**, *39*, 1353−1365.
(39) Monteiro, M. J.; de Brouwer, H. *Macromolecules* **2001**, *34*, 349−352.
(40) Perrier, S.; Barner-Kowollik, C.; Quinn, J. F.; Vana, P.; Davis, T. P. *Macromolecules* **2002**, *35*, 8300−8306.
(41) Barner-Kowollik, C.; Coote, M. L.; Davis, T. P.; Radom, L.; Vana, P. *J. Polym. Sci., Polym. Chem.* **2003**, *41*, 2828−2832.
(42) Wang, A. R.; Zhu, S.; Kwak, Y.; Goto, A.; Fukuda, T.; Monteiro, M. S. *J. Polym. Sci., Polym. Chem.* **2003**, *41*, 2833−2839.

MA050216R